LETTER

doi:10.1038/nature14333

A primordial origin for the compositional similarity between the Earth and the Moon

Alessandra Mastrobuono-Battisti[1], Hagai B. Perets[1] & Sean N. Raymond[2,3]

Most of the properties of the Earth–Moon system can be explained by a collision between a planetary embryo (giant impactor) and the growing Earth late in the accretion process[1–3]. Simulations show that most of the material that eventually aggregates to form the Moon originates from the impactor[1,4,5]. However, analysis of the terrestrial and lunar isotopic compositions show them to be highly similar[6–11]. In contrast, the compositions of other Solar System bodies are significantly different from those of the Earth and Moon[12–14], suggesting that different Solar System bodies have distinct compositions. This challenges the giant impact scenario, because the Moon-forming impactor must then also be thought to have a composition different from that of the proto-Earth. Here we track the feeding zones of growing planets in a suite of simulations of planetary accretion[15], to measure the composition of Moon-forming impactors. We find that different planets formed in the same simulation have distinct compositions, but the compositions of giant impactors are statistically more similar to the planets they impact. A large fraction of planet–impactor pairs have almost identical compositions. Thus, the similarity in composition between the Earth and Moon could be a natural consequence of a late giant impact.

Successful models for Moon formation typically require a relatively low-velocity, oblique impact[1] between the proto-Earth and a planetary embryo of up to a few tenths of an Earth-mass ($M_{\oplus}$). Such Moon-forming impacts typically occur at the late stages of planetesimal accretion by the terrestrial planets[2,3]. A circum-terrestrial debris disk is formed from material ejected during these impacts. The composition of the disk, in a typical impact, is dominated by material from the impactor mantle (>60 weight per cent[1,4,5]) with a smaller contribution (typically about 20%) from the proto-Earth. More material can be extracted from the proto-Earth when a slightly sub-Mars-sized body hits a fast-spinning planet that is later slowed down by resonances[16]. The spin should be close to the break-up velocity. Another possible channel producing such mixing of material from both the planet and impactor is the rare collision between two embryos of comparable mass, in which both masses are about half of the Earth's mass[17]. Although these new models can potentially solve some of the composition issues raised by the giant-impact scenario, they do require *ad hoc* assumptions and pose several difficulties (see ref. 3 for a discussion). Here, we focus on typical giant-impact events, in which the Moon aggregates mostly from material originating from the impactor.

Lunar meteorites and rock samples returned by the Apollo mission have a very similar composition to that of the Earth's mantle, across a variety of different isotopes[6–11]. Combining these with the giant-impact simulation results, one can infer that the Moon-forming impactor and the Earth should have had a similar composition. This poses a fundamental difficulty with the giant-impact model for the origin of the Moon, since analysis of material from other Solar System bodies have shown them to differ significantly (>20σ) in composition from that of the Earth (see refs 12 and 13, and ref. 14 for a review). This would suggest that the composition of the Moon-forming impactor should similarly have differed from that of the Earth, in contrast with the giant-impact basic prediction.

Here, we analyse the results of extensive *N*-body simulations of terrestrial planet formation to show that the Earth–Moon composition challenge can be addressed. In particular, we show that the compositions of a large fraction, 20% to 40%, of giant impactors are consistent with being similar to that of the planets they impact. More generally, late giant impactors have compositions more similar to those of the planets they impact than do other planets in the same system, showing large differences (the probability of these two distributions of coming from the same parent distribution is between 1.3×10^{-9} and 6.7×10^{-8}).

To study the compositions of planets and their impactors we analysed 40 dynamical simulations (from ref. 15, using the Mercury code[18]) of the late stages of planetary accretion, following the formation of Jupiter and Saturn, and after all the gas in the protoplanetary disk has been dissipated and/or accreted to the gas giants (see ref. 19 for a recent review). Each simulation started from a disk of 85–90 planetary embryos and 1,000–2,000 planetesimals extending from 0.5 astronomical units (1 AU is the Earth–Sun distance) to 4.5 AU. Jupiter and Saturn are fully formed and have different orbits and inclinations in different sets of simulations (detailed descriptions can be found in ref. 15 and in the Methods). Within 100–200 million years, each simulation typically produced 3–4 rocky planets formed from collisions between embryos and planetesimals. Each of these planets accreted a large number of planetesimals during its evolution. All collisions were recorded and provide a map of each planet's feeding zone (see also ref. 20). Assuming that the initial composition of material in the protoplanetary disk is a function of its position in the initial protoplanetary disk, one can compare the compositions of different bodies formed and evolved in the simulations.

Previous studies explored the compositions of the different planets formed in similar simulations. However, the compositions of impactors on formed planets have hardly been explored. Pahlevan and Stevenson[21] analysed a single statistically limited simulation, which included a total of about 150 particles, and compared the compositions of any impactors on any planets during the simulation (not only giant impacts, due to small number statistics) to the compositions of the planets. They[21] concluded that the scatter among the compositions of the various impactors is comparable to the observed differences between the planets. In particular, they found that none of the planetary impactors in the simulation they analysed had an isotopic composition similar enough to the final planet to yield a composition similarity such as that of the Earth and the Moon.

Using the data from our large set of high-resolution simulations, we compare the composition of each surviving planet with that of its last giant impactor, that is, the last planetary embryo that impacted the planet (typical impactor-to-planet mass ratio in the range 0.2–0.5; see Table 1). We include only the 20 cases where both the impactor and planet are composed of at least 50 particles each, so as to have sufficient statistics. Analysis of the additional data for impactors composed of a smaller number of particles (and hence having smaller statistics for the specific composition) are consistent with the higher-resolution cases

[1]Department of Physics, Technion, Israel Institute of Technology, Haifa 32000, Israel. [2]CNRS, Laboratoire d'Astrophysique de Bordeaux, UMR 5804, F-33270 Floirac, France. [3]Université Bordeaux, Laboratoire d'Astrophysique de Bordeaux, UMR 5804, F-33270 Floirac, France.

Table 1 | The modelled planet–impactor systems and observations of Solar System bodies

Model	Number	M_P ($M_\oplus$)	M_I ($M_\oplus$)	M_I/M_P	N_P	N_I	t_{coll} (Myr)	$C_{cal} \times \Delta^{17}O$ (p.p.m.)			Kolmogorov–Smirnov probability		
								0%	20%	40%	0%	20%	40%
cjs15	1	0.94	0.43	0.46	123	97	50.7	13 ± 14	10 ± 13	8 ± 12	0.0039	0.13	0.67
cjs15	2	0.78	0.27	0.35	209	78	80.9	$(-1.05 \pm 0.26) \times 10^2$	-84 ± 23	-63 ± 22	1.3×10^{-7}	3.1×10^{-4}	0.079
cjs1	3	1.25	0.42	0.34	219	73	149.7	64 ± 13	52 ± 11	39.9 ± 9.6	5.3×10^{-11}	8.1×10^{-7}	0.0092
cjs1	4	1.05	0.39	0.37	128	78	186.2	$(-1.97 \pm 0.20) \times 10^2$	$(-1.57 \pm 0.20) \times 10^2$	$(-1.18 \pm 0.20) \times 10^2$	1.1×10^{-29}	5.1×10^{-18}	0.052
cjs1	5*	1.21	0.38	0.31	219	75	123.5	-24 ± 17	-20 ± 15	-15 ± 13	0.0023	0.056	0.19
cjsecc	6	0.94	0.36	0.38	117	79	80.4	-51 ± 34	-40 ± 30	-31 ± 27	3.4×10^{-4}	0.025	0.33
cjsecc	7	1.01	0.32	0.32	144	68	75.5	-12 ± 16	-10 ± 13	-7 ± 12	0.038	0.050	0.20
cjsecc	8	1.02	0.42	0.41	148	89	36.9	13 ± 79	11 ± 71	8 ± 66	0.054	0.21	0.53
eejs15	9	0.70	0.19	0.27	111	52	77.1	9.1 ± 7.4	7.3 ± 6.2	5.5 ± 5.2	0.071	0.18	0.32
eejs15	10	0.55	0.13	0.24	263	65	24.6	98 ± 29	78 ± 24	59 ± 22	1.6×10^{-12}	2.3×10^{-8}	0.0025
eejs15	11	0.78	0.22	0.29	256	69	102.3	$(-1.08 \pm 0.35) \times 10^2$	-87 ± 31	-65 ± 27	2.9×10^{-13}	7.9×10^{-7}	0.0069
eejs15	12	0.73	0.26	0.36	298	87	105.6	26 ± 18	21 ± 16	16 ± 14	1.3×10^{-10}	5.5×10^{-6}	0.034
eejs15	13*	1.30	0.33	0.25	525	126	199.8	$93 \pm 1.5 \times 10^2$	$74 \pm 1.3 \times 10^2$	$55 \pm 1.1 \times 10^2$	7.1×10^{-8}	5.4×10^{-6}	0.0043
eejs15	14	0.50	0.18	0.36	170	53	33.1	-26 ± 75	-21 ± 65	-16 ± 56	0.14	0.13	0.24
eejs15	15	0.50	0.13	0.26	234	61	32.0	-73 ± 56	-58 ± 48	-44 ± 43	2.7×10^{-8}	1.8×10^{-7}	0.062
eejs15	16	0.67	0.33	0.49	213	120	145.0	$(1.37 \pm 0.51) \times 10^2$	$(1.10 \pm 0.45) \times 10^2$	83 ± 42	2.4×10^{-5}	0.013	0.43
eejs15	17*	1.15	0.41	0.36	177	69	168.3	$(7.9 \pm 1.3) \times 10^2$	$(6.3 \pm 1.1) \times 10^2$	$(4.75 \pm 0.93) \times 10^2$	3.5×10^{-19}	1.2×10^{-10}	0.0028
ejs15	18	0.81	0.36	0.44	63	55	76.3	-81 ± 48	-65 ± 42	-49 ± 37	1.5×10^{-5}	0.0039	0.29
jsres	19	1.04	0.32	0.31	166	89	79.5	55 ± 22	44 ± 19	33 ± 17	3.0×10^{-10}	1.5×10^{-6}	0.0078
jsres	20	1.27	0.63	0.50	134	89	176.8	-84 ± 29	-67 ± 25	-50 ± 23	5.6×10^{-7}	0.011	0.50
Measured								$\Delta^{17}O$ (p.p.m.)					
Earth		1						0 ± 3					
Moon		0.012						12 ± 3					
Mars		0.07						321 ± 13					
4 Vesta		4.33×10^{-5}						-250 ± 80					

M_P, N_P and M_I, N_I are the mass and number of particles in the planet and the impactor, respectively; t_{coll} is the collision time in the simulations; C_{cal} is the calibration pre-factor (see main text). The $\Delta^{17}O$ composition difference and the Kolmogorov–Smirnov probability (of the distribution of the feeding zones of the planet and impactor being sampled from the same parent distribution) are shown for both the case of no contribution of planetary material to the newly formed Moon, and the cases of 20% and 40% contribution of material from the planet.
* Three-planet systems; calibration was done on the second and third planets.

discussed here, as shown in the Methods. The comparison is then done as follows. First we compare the feeding zones of the planet and impactor, as shown in the examples in Fig. 1 (the cumulative plots for these and all other cases can be found in the Methods). We calculate the probability P that the feeding zones of the impactor and the planet are drawn from the same distribution, using a two-group Kolmogorov–Smirnov test (probabilities shown in the plots and in Table 1). In 3 out of 20 cases the feeding zones contributing to the Moon and those contributing to the planet are consistent with being drawn from the same parent distribution. In other words, the Moon's feeding zones, if derived solely from the impactor, are consistent with the Earth's in 15% of the impacts. The consistency further improves if we assume that a fraction of the proto-Earth was mixed into the Moon (as suggested by detailed collision simulations showing a 10%–40% contribution from the proto-Earth[14]). For the typical 20% mix of proto-Earth material with the impactor material forming the Moon (as found in simulations), 35% of cases are consistent with their feeding zones being drawn from the same parent distribution, and the success rate increases further for a

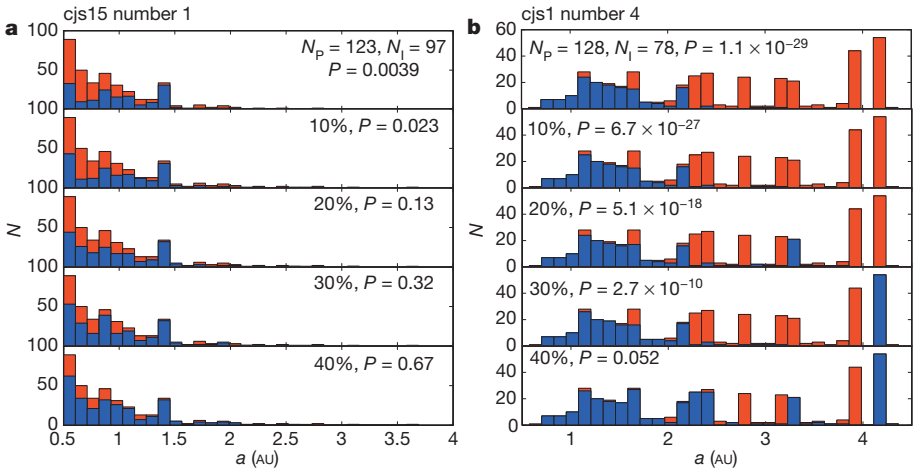

Figure 1 | The distribution of planetesimals composing the planet and the impactor. **a**, A case where the origins of the planetesimals composing the planet (red) and the impactor (blue) are consistent with being sampled from the same parent distribution for the expected typical 20% contribution of planetary material in moon-forming impacts (Kolmogorov–Smirnov test probability >0.05). **b**, A case where the planet and impactor compositions are inconsistent ($P < 0.05$), but become consistent once a large (40%) contribution of material from the planet is considered. The lower plots in each panel show the results when different contributions from the planet are assumed (four cases are shown 10%; 20%; 30% and 40%). The cumulative distribution for these cases as well as all other planet–impactor pairs in Table 1 can be found in the Methods.

higher mass contribution from the proto-Earth (see Table 1 and Extended Data Figs 1 and 2). While this shows that the proto-Earth and the Moon-forming impactor may have had similar feeding zones, it does not yet quantitatively guarantee that the composition is as similar as that of the Earth–Moon system.

We therefore further explore the compositional similarities with the Earth–Moon system, and calculate the oxygen isotope ratios of our simulated planets. We assume that a linear gradient existed in the ^{17}O isotopic composition in the initial protoplanetary disk of the Solar System. Following ref. 21 we calibrate the initial ^{17}O isotopic composition in each of our simulations using the measured compositions of Earth and Mars (see ref. 21 and the Methods, where we also discuss the sensitivity of the results to the calibration used, as well as the criteria for which planet–impactor pairs are considered in the analysis. We find qualitatively similar results when using different criteria and calibrations, as we discuss in detail in the Methods). Given this calibration we assign each planetesimal and planetary embryo a specific initial ^{17}O isotopic abundance based on its initial orbit, and then average the contribution of all accreted planetesimals, while weighting each accreted planetesimal/embryo according to its mass, to obtain the ^{17}O of the planets and impactors and derive the offset between them.

The ^{17}O isotope is chosen for comparison since it provides the most stringent constraint on the Earth–Moon similarity, and its abundances were measured across a variety of Solar System bodies (enabling the best opportunity for calibration). The measured difference between the ^{17}O abundances of Mars and Earth (used for calibration) is $\Delta^{17}O_{Mars} = +321 \pm 13$ parts per million (p.p.m.)[12] (a similarly large difference was found for the composition of 4 Vesta asteroid derived from HED (howardite–eucrite–diogenite) meteorites; -250 ± 80 p.p.m.; ref. 13). The difference between the Earth and Moon is just $\Delta^{17}O = 12 \pm 3$ p.p.m. (ref. 11). In Table 1 we show the $\Delta^{17}O$ differences between the impactors and the planets in our simulations. We adopt the same Earth–Mars composition difference calibration as used by ref. 21. The results are linearly dependent on the adopted calibration; see Table 1. The calibration factor is defined as $C_{cal} = (\Delta^{17}O_4 - \Delta^{17}O_3)/\Delta^{17}O_{Mars}$, where $\Delta^{17}O_4$ and $\Delta^{17}O_3$ refer to the compositions of the fourth and third planet in the simulations (unless only three planets formed, in which case the third and second planet were taken for calibration purposes).

In 20% of the cases the impactors and planets have absolute offsets comparable or smaller than the measured absolute offset in the Earth–Moon system, that is, smaller than the 1σ limit estimated using the lunar samples (<15 p.p.m.). Taking into account the 1σ uncertainty calculated for the $\Delta^{17}O$ in the simulated systems, the fraction of consistent pairs can be as large as 40% of the whole sample. This fraction becomes larger when partial mixing of Earth material is allowed, as observed in simulation data (it increases to 50% for a 20% (and to 55% for a 40%) contribution from the planet; see Table 1 and Fig. 2). Even planet–impactor pairs with statistically different feeding zones have $\Delta^{17}O$ offsets significantly (see Table 1) smaller than those found for Mars and Vesta, in most cases. More generally, planet–impactor pairs are robustly more similar in composition than are pairs of surviving planets in the same system (see Fig. 2 and Extended Data Figs 3, 4 and 5, as well as the Supplementary Table, for the $\Delta^{17}O$ difference distribution for planets and impactors). No less importantly, the differences between the planets are of a similar order to those found between the Earth, Mars and Vesta, that is, consistent with the observations of the Solar System. Interestingly, a small fraction of the planets do have very similar composition (small $\Delta^{17}O$ difference), suggesting the possibility of the existence of Solar System bodies with similar compositions to the Earth besides the Moon. As shown in Extended Data Table 2 and in the Methods, this result still holds when considering lower thresholds for the minimal number of particles composing the planet or impactor (between 1 to 40). In particular, the mean fraction of compatible planet–impactor pairs falls between 10% and 20% for all cases. The fractions become even higher (20%–40%) when accounting for the 1σ uncertainties.

The Earth–Moon composition similarity poses a major challenge to the standard model of the giant-impact scenario because it conflicts with the predominant derivation of the Moon composition from the mantle of the impacting planet[14]. A wide range of alternative impact scenarios were therefore investigated[14,16,17,21–24]. However, all such models suffer from potentially considerable difficulties and/or require fine-tuned conditions (see ref. 14 for a review). Our analysis of Solar-System-like planet formation scenarios potentially offers a solution to the major composition-similarity obstacle to the standard giant-impact scenario. We find that a significant fraction of all planetary impactors could have had compositions similar to the planets they struck, in contrast with the distinct compositions of different planets existing in the same planetary system.

Note that the solution, suggested by our results, of the impactor and planet having a similar composition is also applicable to the origin of the $\Delta^{17}O$ similarity between the Earth and the Moon, and may similarly apply for the isotopic similarities of silicon and tungsten[25]. However, it

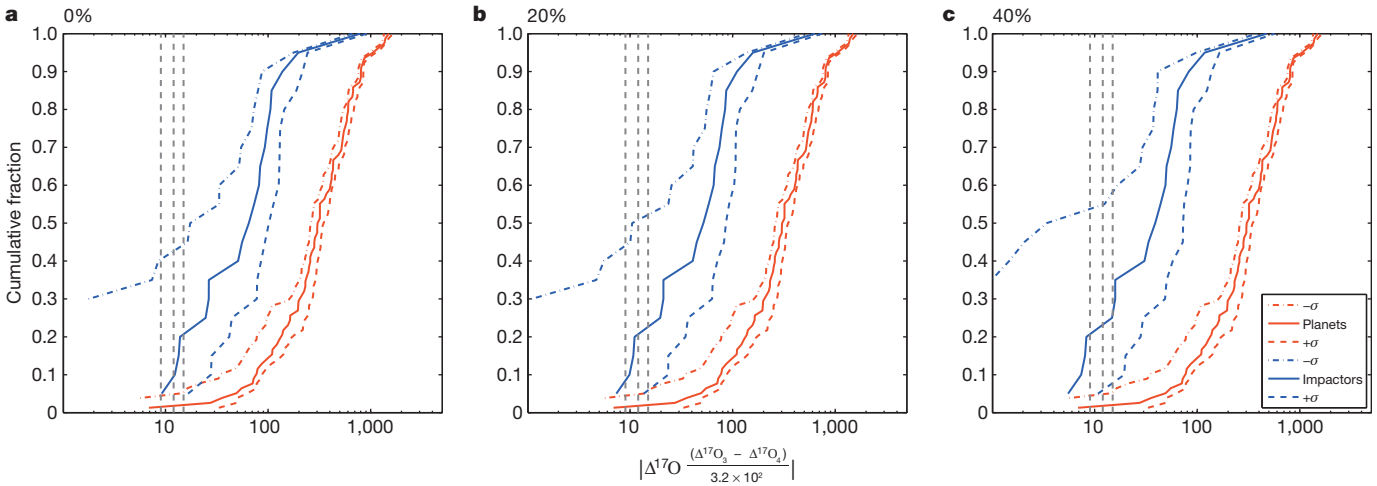

Figure 2 | The cumulative distribution of the absolute $\Delta^{17}O$ differences between planets and their last giant impactors (blue), compared with the differences between planets in the same system (red). Panels **a**, **b** and **c** correspond to the cases of zero, 20% and 40% contribution of material from the planet to a Moon formed from these impacts, respectively. The vertical lines depict the $\Delta^{17}O$ difference of the Earth–Moon system (dashed lines for $\pm\sigma$ around the mean value; central dashed line). The differences between the planet–impactor pairs are systematically smaller than those found between different planets (the same parent distribution for the two groups can be excluded with high confidence; Kolmogorov–Smirnov probability 6.7×10^{-8}, 1.1×10^{-8} and 1.3×10^{-9} for the zero, 20% and 40% cases, respectively).

is debatable whether even a similar impactor–planet composition could resolve the compositional similarity of silicon, given that the Earth's silicate mantle may reflect the consequences of silicon sequestration by a core formed at high temperatures on a large planetary body[25,26], that is, larger than the typical impactors considered.

We conclude that our findings can potentially resolve the apparent contrast between the observed similarity of the Earth and the Moon composition and its difference from that of other Solar System bodies. This primordial composition similarity solution may therefore remove the main obstacle to the standard giant-impact origin of the Moon, as well as ease some of the difficulties for the alternative giant-impact scenarios suggested in recent years[14].

Online Content Methods, along with any additional Extended Data display items and Source Data, are available in the online version of the paper; references unique to these sections appear only in the online paper.

Received 10 November 2014; accepted 10 February 2015.

1. Canup, R. M. & Asphaug, E. Origin of the Moon in a giant impact near the end of the Earth's formation. *Nature* **412,** 708–712 (2001).
2. Agnor, C. B., Canup, R. M. & Levison, H. F. On the character and consequences of large impacts in the late stage of terrestrial planet formation. *Icarus* **142,** 219–237 (1999).
3. Jacobson, S. A. & Morbidelli, A. Lunar and terrestrial planet formation in the Grand Tack scenario. *Phil. Trans. R. Soc. Lond. A* **372,** 20130174 (2014).
4. Canup, R. M. Simulations of a late lunar-forming impact. *Icarus* **168,** 433–456 (2004).
5. Canup, R. M. Lunar-forming collisions with pre-impact rotation. *Icarus* **196,** 518–538 (2008).
6. Ringwood, A. E. Terrestrial origin of the moon. *Nature* **322,** 323–328 (1986).
7. Lugmair, G. W. & Shukolyukov, A. Early solar system timescales according to ^{53}Mn-^{53}Cr systematics. *Geochim. Cosmochim. Acta* **62,** 2863–2886 (1998).
8. Wiechert, U. *et al.* Oxygen isotopes and the Moon-forming giant impact. *Science* **294,** 345–348 (2001).
9. Touboul, M., Kleine, T., Bourdon, B., Palme, H. & Wieler, R. Late formation and prolonged differentiation of the Moon inferred from W isotopes in lunar metals. *Nature* **450,** 1206–1209 (2007).
10. Zhang, J., Dauphas, N., Davis, A. M., Leya, I. & Fedkin, A. The proto-Earth as a significant source of lunar material. *Nature Geosci.* **5,** 251–255 (2012).
11. Herwartz, D., Pack, A., Friedrichs, B. & Bischoff, A. Identification of the giant impactor Theia in lunar rocks. *Science* **344,** 1146–1150 (2014).
12. Franchi, I. A., Wright, I. P., Sexton, A. S. & Pillinger, C. T. The oxygen-isotopic composition of Earth and Mars. *Meteorit. Planet. Sci.* **34,** 657–661 (1999).
13. Clayton, R. N. & Mayeda, T. K. Oxygen isotope studies of achondrites. *Geochim. Cosmochim. Acta* **60,** 1999–2017 (1996).
14. Asphaug, E. Impact origin of the Moon? *Annu. Rev. Earth Planet. Sci.* **42,** 551–578 (2014).
15. Raymond, S. N., O'Brien, D. P., Morbidelli, A. & Kaib, N. A. Building the terrestrial planets: constrained accretion in the inner Solar System. *Icarus* **203,** 644–662 (2009).
16. Ćuk, M. & Stewart, S. T. Making the Moon from a fast-spinning Earth: a giant impact followed by resonant despinning. *Science* **338,** 1047–1052 (2012).
17. Canup, R. M. Forming a Moon with an Earth-like composition via a giant impact. *Science* **338,** 1052–1055 (2012).
18. Chambers, J. E. A hybrid symplectic integrator that permits close encounters between massive bodies. *Mon. Not. R. Astron. Soc.* **304,** 793–799 (1999).
19. Raymond, S. N., Kokubo, E., Morbidelli, A., Morishima, R. & Walsh, K. J. Terrestrial planet formation at home and abroad. In *Protostars and Planets VI* (eds Beuther, H., Klessen, R., Dullemond, C. & Henning, Th.), 585–618 (University of Arizona Press, 2014).
20. Raymond, S. N., Quinn, T. & Lunine, J. I. High-resolution simulations of the final assembly of Earth-like planets. I. Terrestrial accretion and dynamics. *Icarus* **183,** 265–282 (2006).
21. Pahlevan, K. & Stevenson, D. J. Equilibration in the aftermath of the lunar-forming giant impact. *Earth Planet. Sci. Lett.* **262,** 438–449 (2007).
22. Belbruno, E. & Gott, J. R. III. Where did the Moon come from? *Astron. J.* **129,** 1724–1745 (2005).
23. Salmon, J. & Canup, R. M. Lunar accretion from a Roche-interior fluid disk. *Astrophys. J.* **760,** 83 (2012).
24. Reufer, A., Meier, M. M. M., Benz, W. & Wieler, R. A hit-and-run giant impact scenario. *Icarus* **221,** 296–299 (2012).
25. Dauphas, N., Burkhardt, C., Warren, P. & Teng, F.-Z. Geochemical arguments for an Earth-like Moon-forming impactor. *Phil. Trans. R. Soc. Lond. A* **372,** 20130244 (2014).
26. Elliott, T. & Stewart, S. T. Planetary science: shadows cast on Moon's origin. *Nature* **504,** 90–91 (2013).

Supplementary Information is available in the online version of the paper.

Acknowledgements H.B.P. acknowledges support from BSF grant number 2012384, the Minerva Center for Life under Extreme Planetary Conditions, the ISF I-CORE grant number 1829/12 and the Marie Curie IRG 333644 'GRAND' grant. S.N.R. acknowledges funding from the Agence Nationale pour la Recherche via grant ANR-13-BS05-0003-002 (project MOJO). We thank O. Aharonson for remarks on an early version of this manuscript. We thank N. Kaib and N. Cowan for helpful discussions on their related work.

Author Contributions A.M.-B. analysed the simulation data and produced the main results; H.B.P. initiated and supervised the project and took part in the data analysis. S.N.R. provided the simulation data used for the analysis. The paper was written by A.M.-B. and H.B.P. with contributions from S.N.R.

Author Information Reprints and permissions information is available at www.nature.com/reprints. The authors declare no competing financial interests. Readers are welcome to comment on the online version of the paper. Correspondence and requests for materials should be addressed to A.M.B. (amastrobuono@physics.technion.ac.il) and H.B.P. (hperets@physics.technion.ac.il).

METHODS

In the following we supply additional data on the compositions of planet–impactor pairs and the compositions of different planets at the same systems. We also provide more detailed information on the methods used, as well as discuss the sensitivity of our results to the various criteria and calibrations which we applied. The full simulation data used in this work can be provided by the authors upon request.

Initial configuration of Jupiter and Saturn. The simulations analysed here are described in detail in ref. 15. The various simulations explore a range of different initial conditions for the gaseous planets. In particular, in the cjs and cjsecc simulations Jupiter and Saturn are placed on orbits with semimajor axes of 5.45 AU and 8.18 AU and mutual inclination of 0.5°. In cjs the orbits are circular while in cjsecc they are eccentric with $e_{\rm Jupiter} = 0.02$ and $e_{\rm Saturn} = 0.03$. In eejs, Jupiter and Saturn are placed in their current positions (5.25 AU and 9.54 AU), with mutual inclination of 1.5° and larger eccentricities than the observed ones ($e_{\rm Jupiter} = e_{\rm Saturn} = 0.1$ or $e_{\rm Jupiter} = 0.07$ and $e_{\rm Saturn} = 0.08$). In ejs the orbits of Jupiter and Saturn have similar parameters to those observed ($a_{\rm Jupiter} = 5.25$AU and $e_{\rm Jupiter} = 0.05$, $a_{\rm Saturn} = 9.54$ and $e_{\rm Saturn} = 0.06$) with mutual inclination of 1.5°. Finally, in jsres, Jupiter and Saturn are placed at $a_{\rm Jupiter} = 5.43$ AU and $a_{\rm Saturn} = 7.30$ AU with $e_{\rm Jupiter} = 0.005$ and $e_{\rm Saturn} = 0.01$ and with mutual inclination of 0.2°.

The composition difference between planets in the same system. The Supplementary Table shows the Δ^{17}O differences between the different planets (in each system) and the impacted planets analysed in the main text. The full cumulative distribution for these data can be seen in Fig. 2. Note that in the cases where two impacted planets were analysed in the same system, the differences are shown with respect to both the first and second planets.

The cumulative composition distribution of planet–impactor pairs. We used the following procedure to calculate the spatial distribution of the feeding zones (used for Fig. 1, Extended Data Figs 1 and 2 and the Kolmogorov–Smirnov probabilities in Table 1). We extracted the record of planetesimals that constitute the planet and the impactor before the last Moon-forming impact, as well as the planet composition after the collision. To account for the different contributions of particles of different masses we replicated n_i times each particle, where n_i is the ratio between the mass of the ith particle and the minimum mass of the planetesimals. The planetesimal record was then used to produce the distribution of the feeding zones used in our analysis. In cases where contribution of planetary material to the Moon composition was considered, we randomly chose particles from the planet and added them to the planetesimals composing the impactor, where appropriate numbers of particles were taken so as to produce the relevant fractional contribution (for the cases of 10%, 20%, 30% or 40% contribution). We then repeated the same analysis as done for the impactor, with these new mixed impactors.

Δ^{17}O calibration. To calculate the Δ^{17}O ($\equiv \delta^{17}\mathrm{O} - 0.52\delta^{16}\mathrm{O}$) for the planet and impactor pairs we followed the procedure described by ref. 21. To assign specific values of Δ^{17}O to each particle in the simulation we calibrated our simulations with the Solar System observations. We assume a linear gradient of Δ^{17}O with heliocentric distance r

$$\Delta^{17}\mathrm{O}(r) = c_1 r + c_2 \quad (1)$$

where the two free parameters in equation (1) were calibrated by assuming that the third planet formed in the system has the composition of the Earth ($\Delta^{17}\mathrm{O} = 0$‰) and the fourth one has the composition of Mars ($\Delta^{17}\mathrm{O} = +0.32$‰). In cases where only three planets formed (marked with an asterisk in Table 1), we assigned the composition of the Earth and of Mars to the second and third planets in the simulation, respectively. We then mass-averaged over all the $\Delta^{17}\mathrm{O}(r)$ of the planetesimals that accreted to form the Earth. We used the heliocentric distance r as the initial position of each body. We did the same for the planetesimals composing the simulated Mars. In this way we have the system of equations

$$\begin{cases} \dfrac{\sum^{N} m_{i,\oplus}(c_1 r_{i,\oplus} + c_2)}{M_{\oplus}} = 0 \\ \dfrac{\sum^{N'} m_{i,\mathrm{Mars}}(c_1 r_{i,\mathrm{Mars}} + c_2)}{M_{\mathrm{Mars}}} = 0.32 \end{cases}$$

where $r_{i,\oplus}$ and $m_{i,\oplus}$ ($r_{i,\mathrm{Mars}}$ and $m_{i,\mathrm{Mars}}$) are the initial position and mass of the ith planetesimal composing the Earth (Mars) and $M_{\oplus}$ (M_{Mars}) is the final total mass of the Earth (Mars). In this way it has been possible to evaluate the Δ^{17}O value for each planetesimal in the system and thus for all the planets in each system. Given this calibration we evaluate the Δ^{17}O of the planet ($\Delta^{17}\mathrm{O_P}$) and of the last impactor ($\Delta^{17}\mathrm{O_I}$), as the average of the Δ^{17}O of all their respective components, as well as calculated the 1σ s.e.m. for each of these values ($\sigma_{\rm P}$ and $\sigma_{\rm I}$). To check whether or not the planet–Moon system is consistent with the Earth–Moon system we evaluated the difference $\Delta^{17}\mathrm{O_I} - \Delta^{17}\mathrm{O_P}$ and the relative error $\sigma = \sqrt{\sigma_{\rm P}^2 + \sigma_{\rm I}^2}$.

To calculate the Δ^{17}O when a fractional contribution from the planet is included, we added the average Δ^{17}O of the planet and the impactor, each weighted according to the appropriate fractional contribution considered.

To study the sensitivity of our results to the Earth–Mars composition difference calibration used, we also considered lower and higher calibrations, between 0.5 and 1.5 times the Earth–Mars Δ^{17}O difference. We re-analysed the fraction of compatible planet–impactor pairs (that is, producing planet–moon pairs with a composition difference equal or smaller than the Earth–Moon composition difference) for these different calibration factors. The results are summarized in Extended Data Table 1. We find that although the fraction of consistent pairs decreases with the use of a larger difference calibration, as expected, difference calibrations as much as 1.5 times larger than the Earth–Mars difference still give rise to a mean 5% of planet–impactor pairs with similar composition (and 40% within 1σ uncertainty in the simulation compositions), rising to a mean 10% to 20% for the cases of 20% and 40% mixing of the planetary material, respectively. In other words, the results are generally robust to that level and do not dependent on a fine-tuned calibration.

Dependence on the criteria for the chosen planet–impactor pairs. To verify the robustness of our results to different criteria for the choice of planet–impactor pairs used in our analysis we studied two different sets of criteria:

(1) Use all planet–last-impactor pairs, considering smaller thresholds (that is, smaller than the 50-particles threshold considered in the main text) for the number of composing particles (and corresponding masses), but requiring an impactor mass of at least $0.5M_{\rm Mars}$ to ensure a Moon-forming impact. Taking a threshold of 1, 10, 20, 30 and 40 as the minimal number of particles, we find that the general conclusion is unchanged; impactors have compositions more similar to the planets they impact than to other planets in the system. The mean fraction of planet–impactor pairs with similarity comparable to that of the Earth–Moon system is between 10% and 20% in all cases (and up to 40% when considering the 1σ uncertainties), as shown in Extended Data Table 2. Extended Data Figs 3, 4 and 5 show the cumulative distributions of the compositions of planets and last impactors for all the systems, regardless of the number of particles that contributed to their formation, and for a minimum of 10, 20, 40 and 50 particles composing the planet and last impactor. Extended Data Figs 3, 4 and 5 are shown for 0%, 20% and 40% mixing between the material of the planet and impactor.

(2) Consider only last impactors on the third planet. Once we require the impactor to have at least $0.5M_{\rm Mars}$ and be composed of a significant (>20) number of particles, the statistics become too small. When we do not consider a minimal threshold for the number of composing particles, we find that 2 out of 18 (11%; up to about 30% with the 1σ uncertainty in the simulation compositions) planet–impactor pairs with a composition difference equal or smaller than the Earth–Moon system.

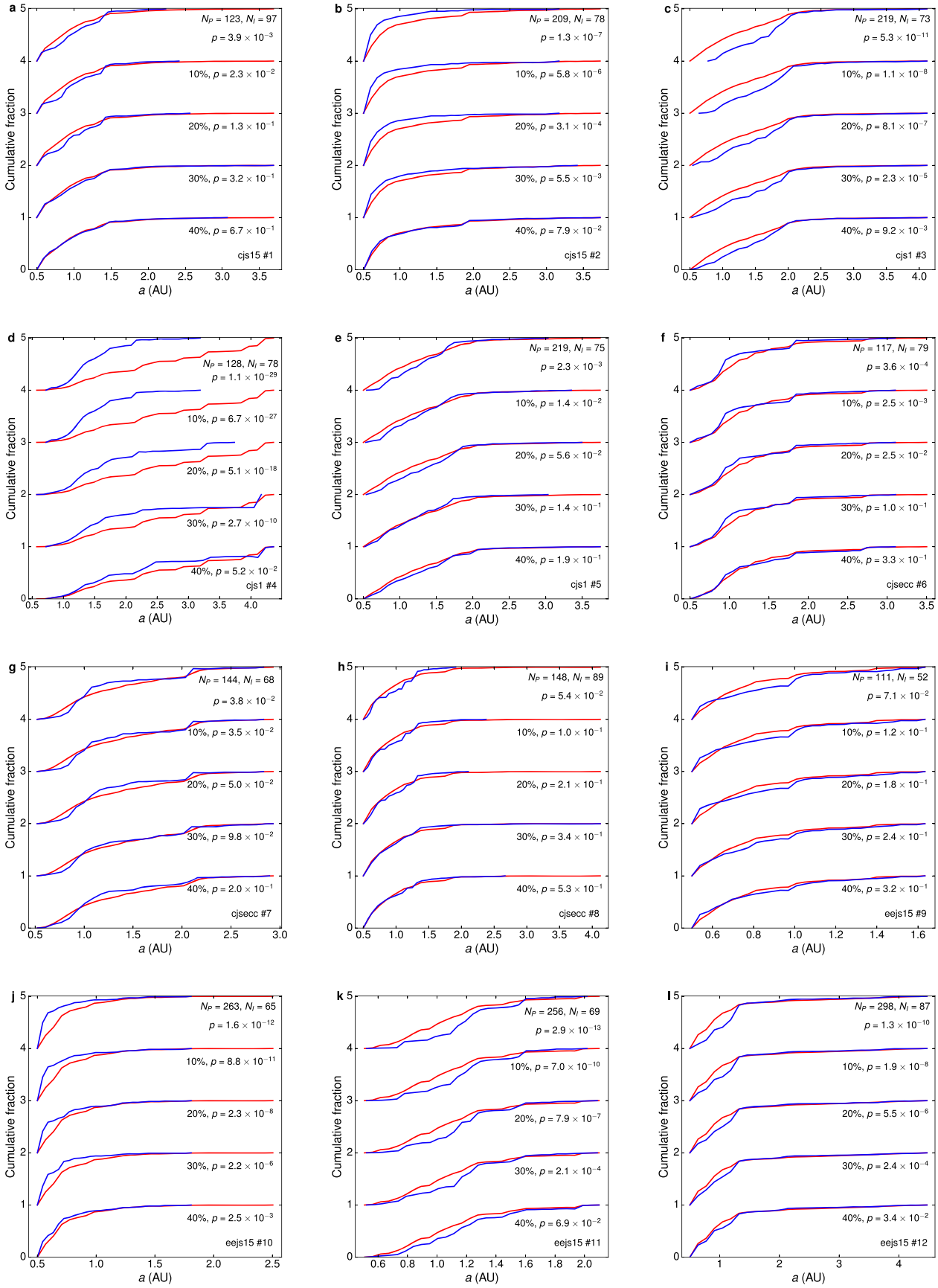

Extended Data Figure 1 | The cumulative distribution of the planetesimals composing the planet (red) and the impactor (blue). All planet–impactor pairs in Table 1 are shown, cases 1–12 (panels **a**–**l**), including the cumulative distributions corresponding to the histograms in Fig. 1.

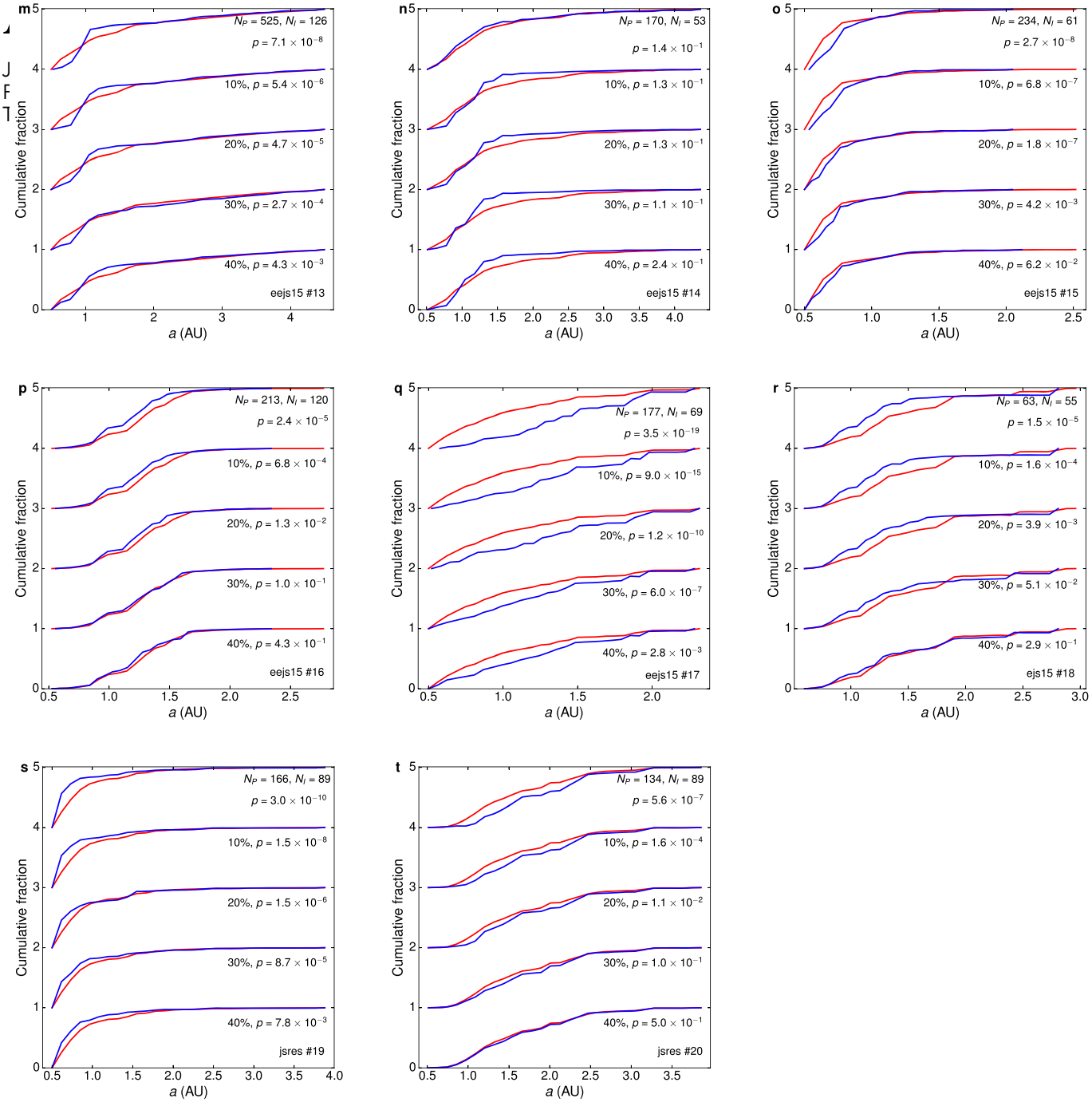

Extended Data Figure 2 | The cumulative distribution of the planetesimals composing the planet (red) and the impactor (blue). All planet–impactor pairs in Table 1 are shown, cases 13–20 (panels **m**–**t**).

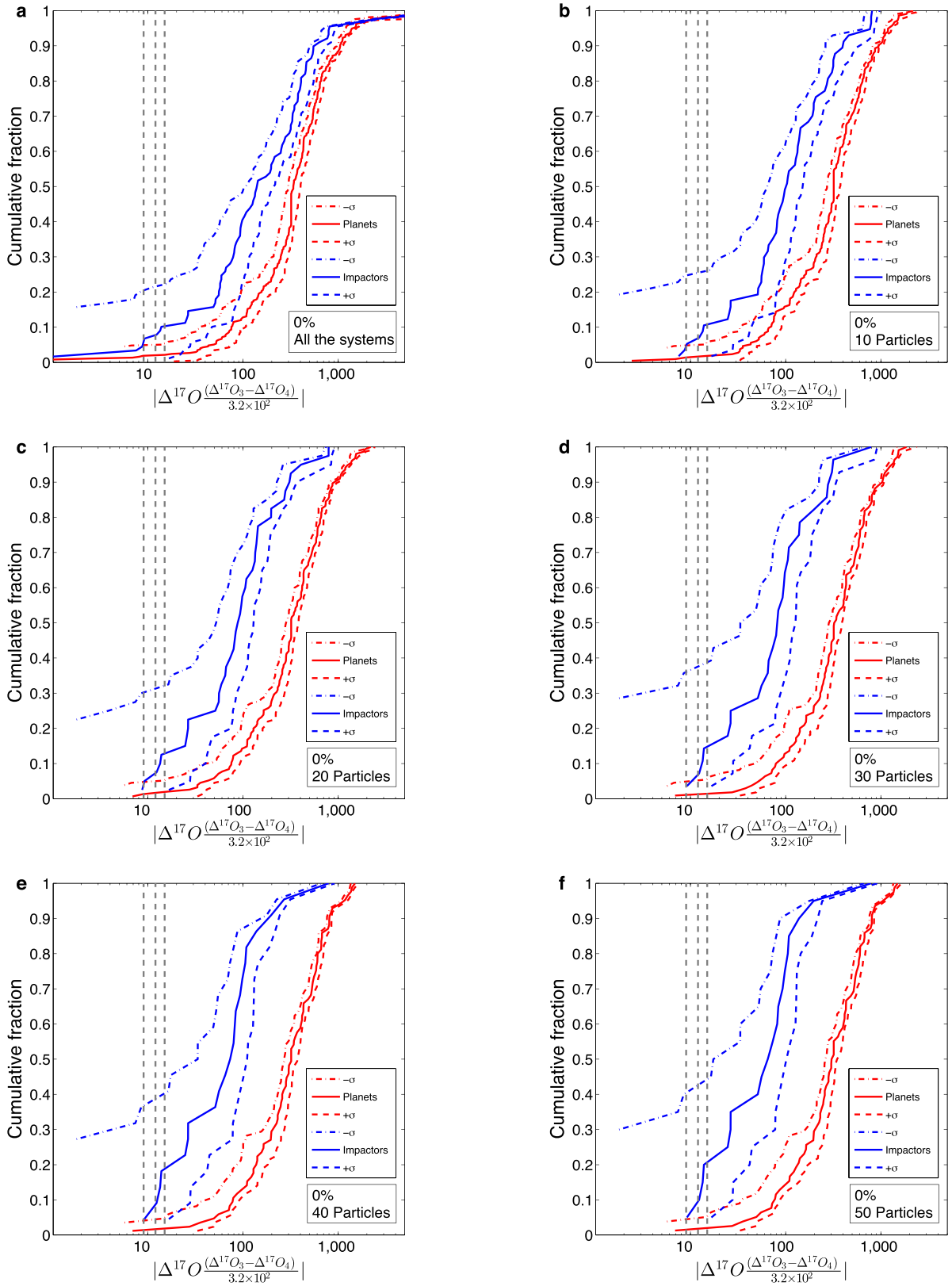

Extended Data Figure 3 | The cumulative distributions of the compositions of planets and last impactors assuming 0% mixing between Earth and Moon material. The cumulative distribution of the absolute Δ^{17}O differences between planets and their last giant impactors (blue), compared with the differences between planets in the same system (red), assuming 0% mixing between Earth and Moon material. From the top left panel (**a**) to the bottom right panel (**f**) we consider all the systems, regardless of the number of particles that contributed to their formation, and planets and last impactors composed of a minimum of 10, 20, 40 and 50 particles. Only last impactors with mass $>0.5M_{\rm Mars}$ have been taken into account.

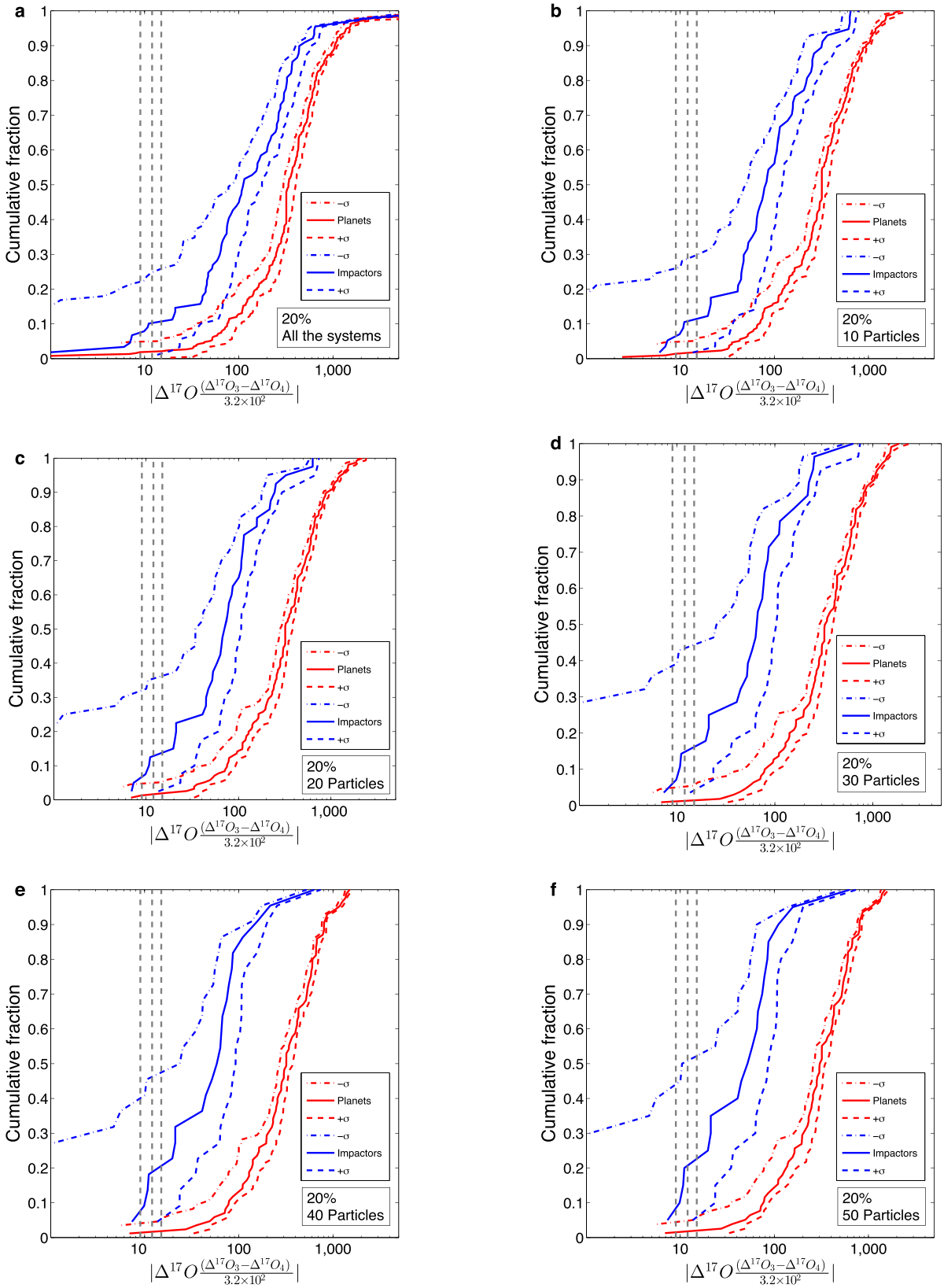

Extended Data Figure 4 | The cumulative distributions of the compositions of planets and last impactors assuming 20% mixing between Earth and Moon material. The cumulative distribution of the absolute $\Delta^{17}O$ differences between planets and their last giant impactors (blue), compared with the differences between planets in the same system (red), assuming 20% mixing between Earth and Moon material. From the top left panel (**a**) to the bottom right panel (**f**) we consider all the systems, regardless of the number of particles that contributed to their formation, and planets and last impactors composed of a minimum of 10, 20, 40 and 50 particles. Only last impactors with mass $>0.5M_{\mathrm{Mars}}$ have been taken into account.

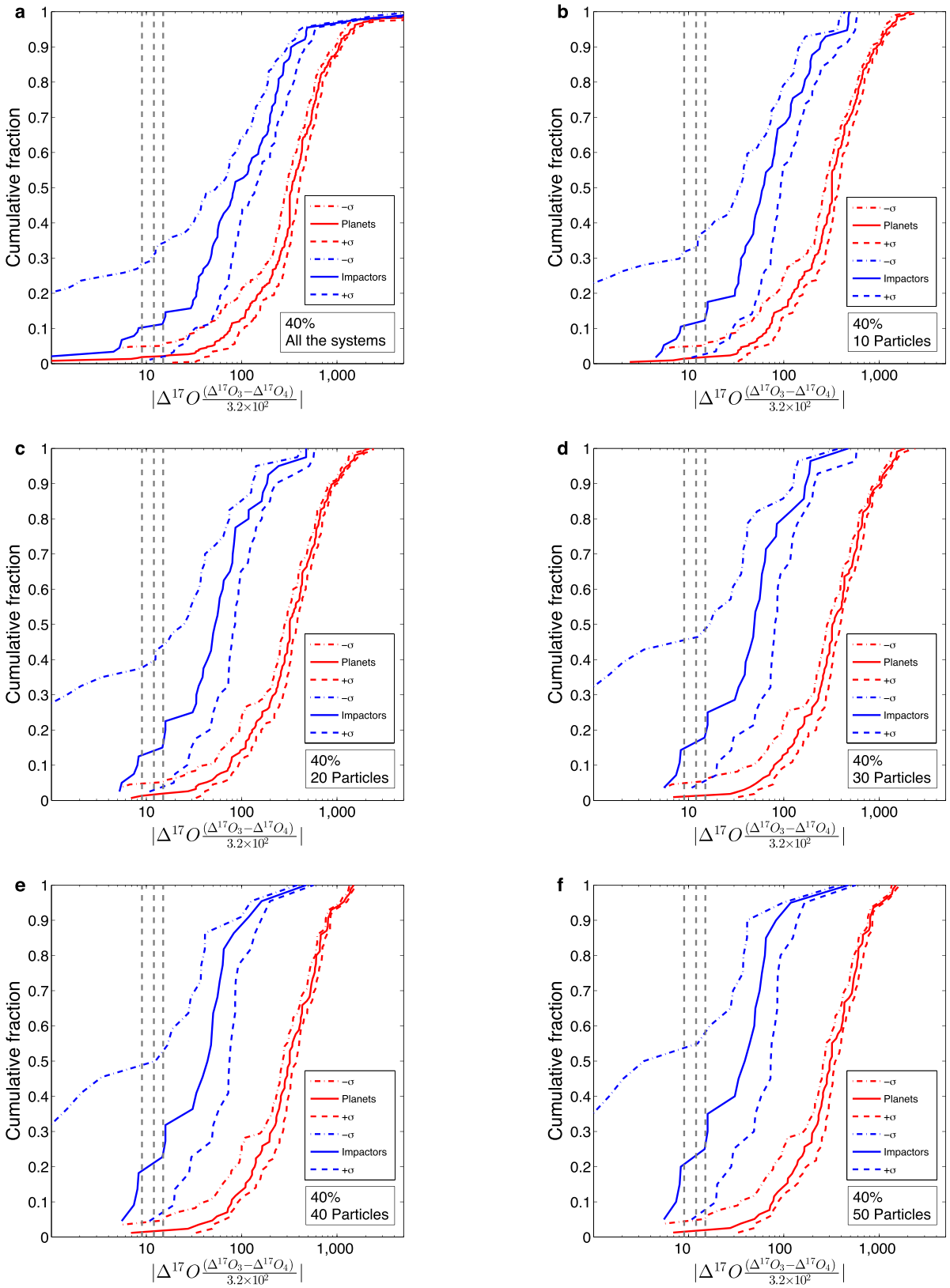

Extended Data Figure 5 | The cumulative distributions of the compositions of planets and last impactors assuming 40% mixing between Earth and Moon material. The cumulative distribution of the absolute $\Delta^{17}O$ differences between planets and their last giant impactors (blue), compared with the differences between planets in the same system (red), assuming 40% mixing between Earth and Moon material. From the top left panel (**a**) to the bottom right panel (**f**) we consider all the systems, regardless of the number of particles that contributed to their formation, and planets and last impactors composed of a minimum of 10, 20, 40 and 50 particles. Only last impactors with mass $>0.5M_{\mathrm{Mars}}$ have been taken into account.

Extended Data Table 1 | The mean fraction of last impactors with a composition compatible with the planet they impact

Factor	0%		20%		40%	
	Mean	1σ	Mean	1σ	Mean	1σ
0.5	35%	50%	35%	60%	35%	70%
0.75	20%	50%	25%	50%	35%	60%
1	20%	40%	20%	50%	25%	55%
1.25	5%	40%	20%	50%	20%	50%
1.5	5%	40%	10%	40%	20%	50%

The fraction is given for different calibration factors and mixing percentages. The pairs which are consistent within 1σ of the simulation uncertainties are also given.

Extended Data Table 2 | The mean fraction of planet–impactor consistent pairs

N_{min}	0%		20%		40%		N_{cases}
	Mean	1σ	Mean	1σ	Mean	1σ	
0	10.1%	21.3%	10.1%	25.8%	11.2%	33.7%	89
10	10.5%	24.6%	10.5%	29.8%	12.3%	36.9%	57
20	12.5%	30%	12.5%	35%	15%	42.5%	40
30	14.3%	35.7%	14.3%	42.9%	17.9%	46.4%	28
40	18.2%	36.4%	18.2%	45.5%	22.7%	50%	22
50	20%	40%	20%	50%	25%	55%	20

The fraction is shown for different mixing percentages (0%, 20%, 40%) and minimum numbers (N_{min}) of the particles composing the impactor and planet (1, 10, 20, 30, 40, 50). The pairs which are consistent within 1σ of the simulation uncertainties are also given. Only the number of cases N_{cases} in which the last impactor has a mass $>0.5M_{Mars}$ have been taken into account.